Optical Engineering

OpticalEngineering.SPIEDigitalLibrary.org

Real-time measurement of the average temperature profiles in liquid cooling using digital holographic interferometry

Carlos Guerrero-Mendez
Tonatiuh Saucedo Anaya
M. Araiza-Esquivel
Raúl E. Balderas-Navarro
Said Aranda-Espinoza
Alfonso López-Martínez
Carlos Olvera-Olvera

SPIE.

Carlos Guerrero-Mendez, Tonatiuh Saucedo Anaya, M. Araiza-Esquivel, Raúl E. Balderas-Navarro, Said Aranda-Espinoza, Alfonso López-Martínez, Carlos Olvera-Olvera, "Real-time measurement of the average temperature profiles in liquid cooling using digital holographic interferometry," *Opt. Eng.* **55**(12), 121730 (2016), doi: 10.1117/1.OE.55.12.121730.

Real-time measurement of the average temperature profiles in liquid cooling using digital holographic interferometry

Carlos Guerrero-Mendez,[a,b,*] Tonatiuh Saucedo Anaya,[b] M. Araiza-Esquivel,[a] Raúl E. Balderas-Navarro,[c] Said Aranda-Espinoza,[d] Alfonso López-Martínez,[a] and Carlos Olvera-Olvera[a]

[a]Universidad Autónoma de Zacatecas, Unidad Académica de Ingeniería Eléctrica, Av. Ramón López Velarde 801, Zacatecas C.P. 98000, México
[b]Universidad Autónoma de Zacatecas, Unidad Académica de Física, Calzada Solidaridad Esq. Con Paseo La Bufa S/N, Zacatecas C.P. 98060, México
[c]Instituto de Investigación en Comunicación Óptica (IICO-UASLP), Avenue Karakorum 1470, Lomas 4ta. Sección, San Luis Potosí C.P. 78210, México
[d]Universidad Autónoma de San Luis Potosí, Instituto de Física, Avenue Salvador Nava 6, Zona Universitaria, San Luis Potosí C.P. 78290, México

Abstract. We present an alternative optical method to estimate the temperature during the cooling process of a liquid using digital holographic interferometry (DHI). We make use of phase variations that are linked to variations in the refractive index and the temperature property of a liquid. In DHI, a hologram is first recorded using an object beam scattered from a rectangular container with a liquid at a certain reference temperature. A second hologram is then recorded when the temperature is decreased slightly. A phase difference between the two holograms indicates a temperature variation, and it is possible to obtain the temperature value at each small point of the sensed optical field. The relative phase map between the two object states is obtained simply and quickly through Fourier-transform method. Our experimental results reveal that the temperature values measured using this method and those obtained with a thermometer are consistent. We additionally show that it is possible to analyze the heat-loss process of a liquid sample in dynamic events using DHI. [DOI: 10.1117/1.OE.55.12.121730]

Keywords: digital holographic interferometry; refractive index difference; liquids temperature; phase difference.

Paper 160626SS received Apr. 26, 2016; accepted for publication Oct. 6, 2016; published online Oct. 27, 2016.

1 Introduction

The thermal conditions of liquid samples are of interest in many areas of science, and determining the temperature of liquid substances is very important in engineering applications, such as the design of air-conditioning units, heat transfer equipment, machines and industrial processes, and thermal energy storage systems.[1] The temperature values of substances are commonly determined using devices that must be in contact with the specimen. However, these devices often affect the dynamic evolution or the mechanical properties of the fields of temperature in a substance. In contrast, common optical techniques are noninvasive, noncontact, and nondestructive, and they have been developed for this purpose using the thermo-optical effect,[2] which is thermal modulation of the refractive index n of a material.[3] However, they only obtain temperature data over a small region of the sample.[4,5]

New advanced optical techniques are more precise and higher resolution, and yield stable full-field measurements between optical fields; these techniques are generally preferred for monitoring the dynamic evolution of entire optical fields. Some of these methods include the Schlieren, shadowgraph, and interferometry techniques.[6] Digital holographic interferometry (DHI) is an optical metrology technique based on holography that records and reconstructs wavefronts to interferometrically compare two or more wavefronts obtained at different moments or states of an object using a computer. Furthermore, DHI is a fast, simple, high-precision, nondestructive, full-field optical technique for measuring variations of physical properties of phase objects in dynamic processes.[7–9]

Some new studies based on DHI have obtained measurements of phase differences and used these data to visualize and determine how flow fields change constantly in both time and space. Several authors have established a physical model to determine a relationship between the phase and the parameter to be analyzed.[10] These investigators have obtained measurements of the temperature variation in fluids,[11] flames,[12–16] and liquids.[11,17–23] However, these methods use the entire wrapped phase map difference or a part of this phase map, and also necessitate a robust algorithm to unwrap the phase map to obtain a physical parameter. Other DHI methods obtain measurements of a phase variation linked with a punctual value of concentration in the crystallization evolution process,[10,24,25] but they neglect the temperature values in their mathematical expressions.

We present an alternative method to measure the temperature of transparent, nonscattering liquid samples. Using a physical model to determine the relation between the phase difference and the temperature variation between a certain time of sample and a reference temperature, we can calculate the temperature value at each point of the liquid sample. The wrapped phase difference map between a

*Address all correspondence to: Carlos Guerrero-Mendez, E-mail: capacti@gmail.com

0091-3286/2016/$25.00

reference-state hologram and a subsequent hologram is calculated digitally using the Fourier-transform method[26] from a series of holograms recorded dynamically between the different states of the liquid sample. This method does not necessitate the entire wrapped phase map, big region, or a line of it to approximate the temperature value in the liquid sample. The temperature values are obtained from the phase variations in a single pixel in the wrapped phase map and an initial temperature value. Furthermore, to increase the accuracy of the method, the dependence of the refractive index on the temperature (i.e., the thermo-optic coefficient of the sample) is considered. Our results reveal that our proposed method is a fast and simple technique that is highly precise, nondestructive, and does not necessitate contact for measuring the temperature evolution in a liquid sample.

2 Experimental Setup and Theory

Figure 1 shows the optical setup for monitoring the cooling process in a liquid sample using DHI. Monochromatic He–Ne laser light at a wavelength of $\lambda = 543.5$ nm and a maximum output power of 5 mW is split into two beams by a plane 50:50 beam splitter BS1. The reflected beam (object beam) from the mirror is sent to a 10× microscope objective MO1 and a lens L1 to expand and collimate the object beam. A diffuser D1 (2.0 mm and 120 grit) creates a diffused illumination that avoids concentric ring patterns that arise from dust particles or scratches on the optical elements. Then the diffused light passes through a transparent quartz cell $10 \times 10 \times 50$ mm ($L \times W \times H$) filled with the hot liquid sample S. The light scattered by the liquid container is modulated by the rectangular aperture A1 in their spatial frequencies, and it passes through this aperture. Next, the modulated light is collected by a positive lens L3 with a focal length of 75 mm. Then the object beam interferes with the transmitted beam (reference beam) in the cubic 50:50 beam splitter BS2 placed in front of a charge-coupled device (CCD). A1 has a size of $\sim 2.31 \times 6.35$ mm ($H \times V$), and the rectangular shape of the aperture is the most convenient because we improve the light collection and obtain higher spatial frequencies, which leads to increased spatial resolution. Furthermore, the Fourier method ensures easy filtering and the possibility of using the maximal area in the CCD.[27,28] A similar microscope objective to MO1 and a lens to L1 are introduced, respectively, as

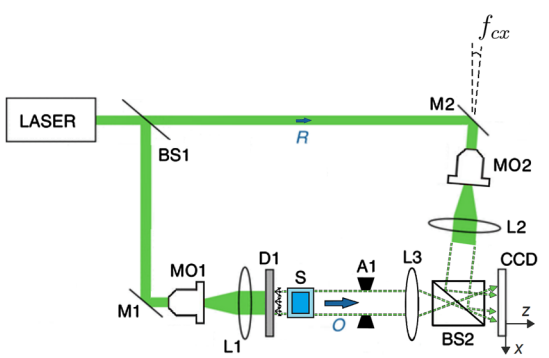

Fig. 1 Schematic diagram of the experimental setup using DHI. BS1: plane beam splitter; BS2: cubic beam splitter; M1, M2: mirrors; MO1, MO2: 10× microscope objectives; L1, L2, L3: lenses; D1: diffuser; S: transparent quartz cell with sample; A1: rectangular aperture; CCD: charge-coupled device; f_{cx}: the spatial carrier frequency along the x direction of the sensor plane; O: object beam; R: reference beam.

MO2 and L2 (to expand and collimate the reference beam) to interfere the reference beam and the object beam intoBS2. A small angle is introduced between the object and the reference beam on the Mach–Zehnder configuration to achieve the off-axis holography geometry. The CCD camera (pco. pixelfly usb) is a monochromatic type with a 14-bit dynamic range with 1392×1040 pixels ($H \times V$) and a pixel size of 6.45×6.45 μm that records the holograms at 12 frames per second (fps). The interference pattern recorded onto the CCD is used to estimate the phase of the object wavefront and later calculate the phase difference between two object beams. For the phase difference calculation, we never reconstructed a complete wavefront as in common digital holography.

2.1 *Phase Estimation*

The holographic technique is able to record the amplitude and phase information of a wavefront that is scattered by a phase object. The total light intensity in the CCD can be expressed as

$$I(x,y) = |O(x,y) + R(x,y)|^2, \tag{1}$$

where

$$O(x,y) = o(x,y)\exp[i\phi(x,y)], \tag{2}$$

and

$$R(x,y) = r(x,y)\exp[-2\pi i(f_{cx}x + f_{cy}y)], \tag{3}$$

are the complex amplitudes of the object and the reference beams, respectively. x and y are rectangular coordinates at the image sensor plane. f_{cx} and f_{cy} represent the spatial carrier frequency along the directions x and y, respectively, due to a small inclination of the reference beam with respect to the system optical axis z.

According to DHI, two holograms generated by an object in two different states or different time lapses t are required to measure a physical variation during a physical process. The object beam of a hologram captured at a specific time $t = 1, 2, 3, \ldots, N$ (where N is the last period of time in the dynamic process) can be represented as

$$O_t(x,y,t) = o_t(x,y,t)\exp[i\phi_t(x,y,t)]. \tag{4}$$

The object beam at an initial time ($t = 0$) is expressed as

$$O_0(x,y,0) = o_0(x,y,0)\exp[i\phi_0(x,y,0)]. \tag{5}$$

The terms ϕ_t and ϕ_0 (phases) can be extracted from an interference pattern, and those phases can be used to create a phase difference $\Delta\phi_{t-0}$ and calculate a physical variation in a dynamic process. For this interference pattern, a valid expression of Eq. (1) can be written as

$$I(x,y) = a(x,y) + c(x,y)\exp[2\pi i(f_{cx}x + f_{cy}y)] + c^*(x,y)\exp[-2\pi i(f_{cx}x + f_{cy}y)], \tag{6}$$

with

$$a(x,y) = o^2(x,y) + r^2(x,y), \tag{7}$$

and

$$c(x,y) = o(x,y)r(x,y)\exp[i\phi(x,y)], \tag{8}$$

where the two last terms of Eq. (6) have a spatial carrier frequency f_{cx} and f_{cy} [see Eq. (3)] that modulates the phase of $O(x,y)$ [Eq. (2)].

Next, we employ the Fourier transform (FT) on Eq. (6) to obtain

$$\begin{aligned}\mathrm{FT}\{I\} = {} & A(f_x,f_y) + C(f_x - f_{cx}, f_y - f_{cy}) \\ & + C^*(f_x - f_{cx}, f_y - f_{cy}),\end{aligned} \tag{9}$$

where the capital letters represent the FT of each term and * denotes the conjugate complex. Any part of the complex term reconstructed wavefront C or C^* in the Fourier spectrum plane is used to calculate $\phi(x,y)$ of the object wavefront. The three different contributions of the reconstructed hologram are spatially separated according to the shape and size of the aperture A1 and the spatial carrier frequencies f_{cx} and f_{cy}. Figure 2 shows the Fourier spectrum as a function of the aperture A1, f_{cx}, and f_{cy} in the optical system in Fig. 1.

The process to calculate $\phi(x,y)$ in Eq. (6) continues by filtering C, and its inverse FT is calculated in order to determine the phase as

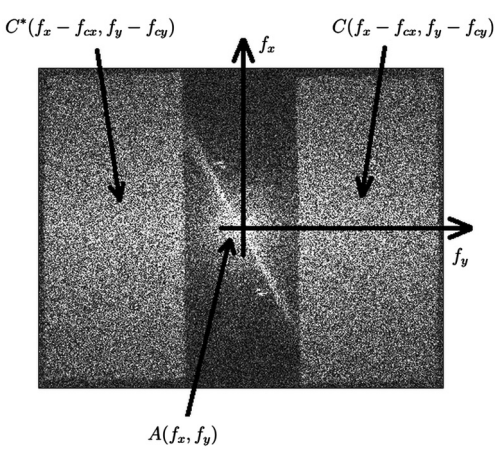

Fig. 2 Fourier spectrum with the aperture A1.

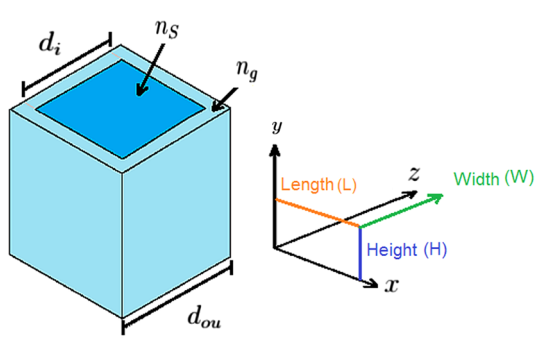

Fig. 3 Rectangular container. d_i and d_{ou} are the inner and outer side lengths of the container, respectively; n_S and n_g are the refractive indices of the liquid sample and the glass walls, respectively. The cell's dimensions are $10 \times 10 \times 50$ mm ($L \times W \times H$).

$$\phi(x,y) + 2\pi i(f_{cx}x + f_{cy}y) = \arctan\frac{\mathrm{Im}[c(x,y)]}{\mathrm{Re}[c(x,y)]}. \tag{10}$$

3 Temperature Determination

In order to measure and study the temperature evolution in a liquid between two different states of a sample using DHI, we need to remotely and noninvasively compare a reference state (a first wave object) with a second state (different wave object) when the liquid temperature decreases. For the case of a rectangular quartz container (see Fig. 3), we obtain a phase distribution according to the optical path length (OPL), the refractive indices of the liquid sample n_S and the container material n_g, and the inner d_i and outer d_{ou} side lengths of the container.[7–9,20]

A phase variation $\Delta\phi_{t-0}$ between the two object wavefronts depends on the variations of the OPL, ΔOPL, and can be expressed as

$$\Delta\phi_{t-0}(x,y) = \frac{2\pi}{\lambda}\Delta\mathrm{OPL} = \frac{2\pi}{\lambda}\int_0^{d_i}[n_{S_t}(x,y,t) - n_{S_0}]\mathrm{d}z, \tag{11}$$

where $n_{S_t}(x,y,t)$ is the refractive index distribution at time t, and n_{S_0} is the refractive index at an initial time or reference state. The object beam passes along the z direction through the liquid sample, and the integration of the refractive indices is taken along the propagation direction z. In an approximation of a temperature variation in a liquid, the phase map difference corresponds to an integration of refractive index variation in the transparent object and is given by

$$\Delta\phi_{t-0}(x,y) = \frac{2\pi}{\lambda}d_i(x,y)[\Delta n_{S_{t-0}}(x,y)]. \tag{12}$$

The interference phase distributions are calculated by modulo 2π subtraction as[17]

$$\Delta\phi_{t-0}(x,y) = \begin{cases}\phi_t(x,y) - \phi_0(x,y) + 2\pi, & \text{if } \phi_t(x,y) - \phi_0(x,y) < -\pi \\ \phi_t(x,y) - \phi_0(x,y) - 2\pi, & \text{if } \phi_t(x,y) - \phi_0(x,y) \geq +\pi \\ \phi_t(x,y) - \phi_0(x,y), & \text{else.}\end{cases} \tag{13}$$

The refractive indices $n_{S_t}(x,y,t)$ and n_{S_0} in Eq. (11) are related to a variation in temperature and/or a concentration of the liquid sample. Therefore, a refractive index difference also can be expressed as[24]

$$\begin{aligned}\Delta n_{S_{t-0}}(x,y) = {} & \left[\frac{\partial n_S}{\partial T}\right]_{\mathrm{Con}}[T_t(x,y) - T_0(x,y)] \\ & + \left[\frac{\partial n_S}{\partial \mathrm{Con}}\right]_T[\mathrm{Con}_t(x,y) - \mathrm{Con}_0(x,y)],\end{aligned} \tag{14}$$

where $T_t(x,y)$ and $\mathrm{Con}_t(x,y)$ are the temperature and the solution concentration at t, respectively; $T_0(x,y)$ and $\mathrm{Con}_0(x,y)$ are the temperature and the solution concentration at $t = 0$; $[(\partial n_S/\partial T)]_{\mathrm{Con}}$ and $[(\partial n_S/\partial \mathrm{Con})]_T$ are the dependence of the refractive index on the temperature and the concentration of S, respectively. If the liquid solution concentration is constant at two times, Eq. (14) can be rewritten as

$$\Delta n_{S_{t-0}}(x,y) = \left[\frac{\partial n}{\partial T}\right]_{Con}[T_t(x,y) - T_0(x,y)]. \quad (15)$$

By substituting Eq. (15) into Eq. (12), we can obtain an expression to calculate the temperature in the full-field distribution at t:

$$T_t(x,y) = T_0(x,y) + \left[\frac{\Delta\phi_{t-0}(x,y)}{d_i(x,y)}\frac{\lambda}{2\pi}\right] / \left[\frac{\partial n_S}{\partial T}\right]_{\text{Con}}. \quad (16)$$

4 Results

Using a reference temperature $T_0(x,y)$ and a small region of series of wrapped phase differences [created with Eq. (13)], we are able to determine the temperature in that small region. Additionally, we can create a one-dimensional (1-D) graph of the temperature evolution in the sample using each small point in it.

In order to verify the correct operation of the experimental setup, we calculated the temperature and visualized the cooling process in distilled water using Eq. (16). We compared this temperature with measurements from a digital thermometer with an accuracy of ±1°C. Furthermore, we used this thermometer to determine the reference temperature $T_0(x,y)$. The parameter $[(\partial n_S/\partial T)]_{\text{Con}}$ in Eq. (16) for distilled water is 0.0001.[29]

As an experimental study, the cell in the schematic setup (see Fig. 1) was filled with 0.66 ml of heated distilled water at 22.0°C. To monitor the cooling process, 1460 holograms were registered at 12 fps; the first hologram reconstructed the initial object wavefront $O_0(x,y,0)$, and the other holograms represented the following time or $O_t(x,y,t)$. The temperature within the laboratory was stabilized at 19°C during the course of experiment. To improve the sensitivity and the results, we used a camera with 14 bits of dynamic range instead of a camera with 8 bits of dynamic range.

We obtained the two-dimensional (2-D) wrapped phase difference distribution using Eq. (13) according to the phase difference between the wavefronts $O_0(x,y,0)$ and $O_t(x,y,t)$. Some of the 2-D wrapped phase differences of the cooling process are shown in Figs. 4(a)–4(f) with $t = 1$, 21, 43, 64, 86, and 108 s, respectively. To verify the method, we obtained a measurement of the phase variations at three points [their dimensions were p1 (4.1 × 2.8 mm), p2 (8.3 × 6.7 mm), and p3 (6.8 × 4.8 mm) on the 2-D wrapped phase differences; see the "x" in Fig. 4]. However, we are also capable of performing temperature measurements over the full field of the phase variation over the entire liquid sample. Since the wrapped phase maps were noisy, we incorporated an averaging filter with a 5 × 5 window to reduce the inherent speckle noise from the interference phase maps (see Fig. 4), but the temperature data were obtained from the raw wrapped phase maps.

We selected the points p1, p2, and p3 near the thermometer to obtain similar temperature data compared with the temperature values obtained using this alternative method. We generated a 1-D wrapped phase graph using the phase difference [Eq. (13)] values at each point (p1, p2, and p3) of the holograms at their respective time of the cooling process. The 1-D wrapped phase graph is shown in Fig. 5(a). Later, we obtained an unwrapped phase value using the 1-D wrapped phase. We used the reference temperature value and every phase increment during a certain t to calculate the liquid temperature in each point using Eq. (16) [see Fig. 5(b)].

Table 1 lists the values obtained with a thermometer and the values obtained with DHI; the deviation between the values is also listed. According to the results, the largest deviation between the three points and the data measured using the thermometer was 0.2°C.

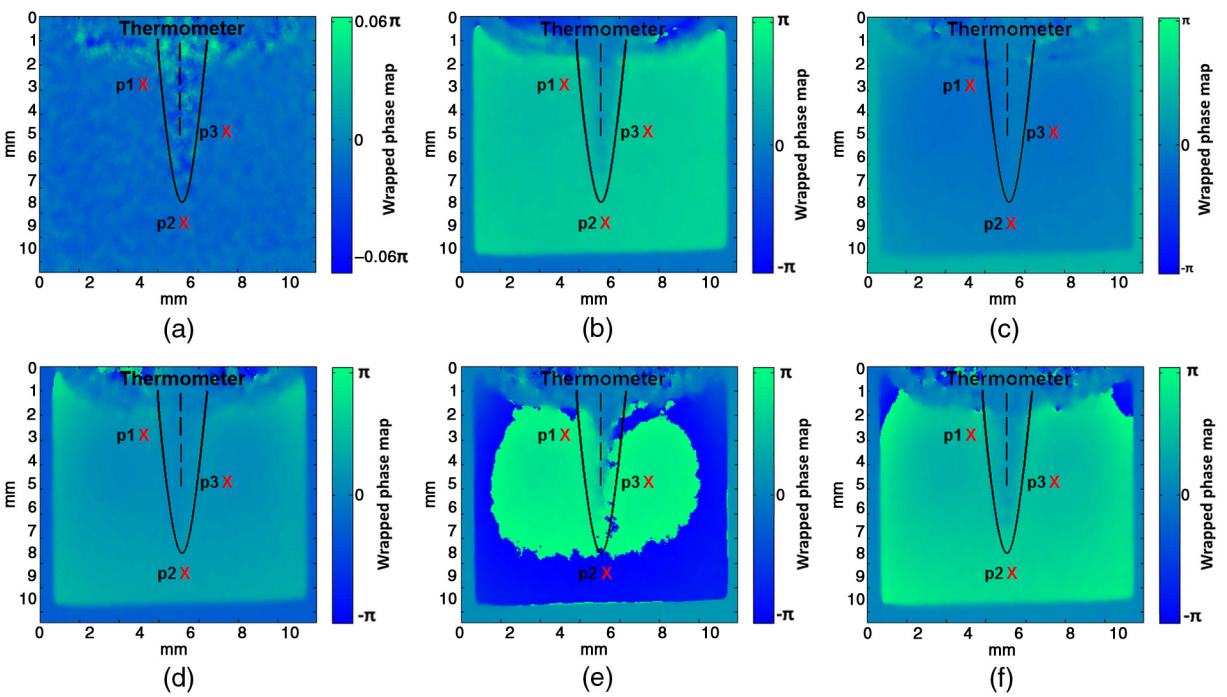

Fig. 4 Wrapped phase difference maps obtained with Eq. (16) showing temperature variations of the distilled water at different times: (a) $t = 1$ s; (b) $t = 21$ s; (c) $t = 43$ s; (d) $t = 64$ s; (e) $t = 86$ s; and (f) $t = 108$ s.

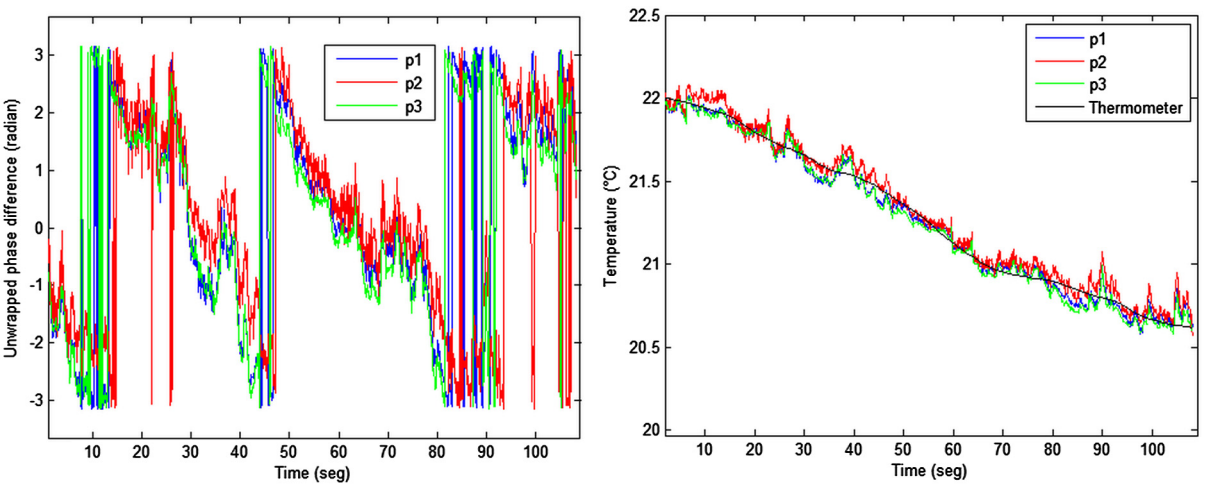

Fig. 5 Phase variation in the pixels p1, p2, and p3: (a) The 1-D wrapped phase obtained at the points and (b) the temperature values at each point.

Table 1 Comparison of temperature values.

Time (s)	Thermometer (°C)	Temperature in p1 (°C)	Temperature in p2 (°C)	Temperature in p3 (°C)	Deviation (°C)
0	22.0	22.0	22.0	22.0	0
1	22.0	21.9	22.0	21.9	0.1
21	21.7	21.8	21.7	21.7	0.1
43	21.4	21.3	21.4	21.3	0.1
64	20.9	20.9	20.9	20.9	0
86	20.8	20.8	20.8	20.7	0.1
106	20.6	20.6	20.5	20.4	0.2

According to our experiments and Newton's law,[30] we confirm that the magnitude of the temperature variation decreases when the final temperature approaches the environmental temperature.

5 Conclusions

We have presented an optical setup to obtain real-time measurements of temperature values during the cooling process of a liquid using DHI. Each pixel in the recorded holograms yields information about the dynamic evolution of the temperature property. Using only the variation of a single pixel in the 2-D wrapped phase difference map and a reference temperature, we can determine the temperature; we do not need the entire phase difference map to obtain one value. Since we possessed full-field information, it was possible to measure the temperature in each pixel in the figure of the hologram. Therefore, the proposed optical technique can detect small changes in temperature on the order of $\pm 0.2^{\circ}$C in distilled water. In as much as DHI is an optical technique, we can obtain noncontact, nondestructive, noninvasive, and full-field temperature values. This situation is in contrast to traditional methods of temperature measurement such as those using thermometers. Our method can be used to study the thermal properties of phase-change materials and to predict the thermal behavior or a phase change of a liquid using only a pixel and its subsequent values.

Acknowledgments

One of the authors (Carlos Guerrero-Mendez) acknowledges CONACYT (México) for providing partial financial support for this work.

References

1. I. Dincer and M. A. Rosen, *Thermal Energy Storage: Systems and Applications*, 2nd ed., John Wiley & Sons, West Sussex (2011).
2. T. S. El-Bawab, *Optical Switching*, Springer Scienee+Business Media, New York (2006).
3. F. T. S. Yu, *Optical Information Processing, Illustrated Reprint.*, R. E. Krieger Publishing Company, Pennsylvania (1990).
4. J. D. Trolinger, "The holography of phase objects," *Proc. SPIE* **1986**, 128–139 (1987).
5. G. R. Toker, *Holographic Interferometry: A Mach–Zehnder Approach*, CRC Press, Boca Raton (2012).
6. R. Golstein, *Fluid Mechanics Measurements*, 2nd ed., CRC Press, Philadelphia (1996).
7. J. Colombani and J. Bert, "Holographic interferometry for the study of liquids," *J. Mol. Liq.* **134**(1), 8–14 (2007).
8. C. M. Vest, *Holographic Interferometry*, Wiley, Michigan (1979).
9. T. Kreis, *Handbook of Holographic Interferometry: Optical and Digital Methods*, Wiley-VCH, Bremen (2006).
10. C. Yang et al., "Dynamic measurement via laser interferometry: crystal growth monitoring and modal parameter analysis," *Proc. SPIE* **9302**, 93021V (2015).
11. J. Zhao et al., "Visual and dynamic measurement of temperature fields by use of digital holographic interferometry," *Proc. SPIE* **8788**, 878828 (2013).
12. S. Sharma, G. Sheoran, and C. Shakher, "Investigation of temperature and temperature profile in axi-symmetric flame of butane torch burner using digital holographic interferometry," *Opt. Lasers Eng.* **50**(10), 1436–1444 (2012).
13. B. Wu et al., "Visual investigation on the heat dissipation process of a heat sink by using digital holographic interferometry," *J. Appl. Phys.* **114**(19), 193103 (2013).
14. R. Doleček et al., "General temperature field measurement by digital holography," *Appl. Opt.* **52**(1), A319–A325 (2013).
15. S. Sharma, G. Sheoran, and C. Shakher, "Digital holographic interferometry for measurement of temperature in axisymmetric flames," *Appl. Opt.* **51**(16), 3228–3235 (2012).
16. J. Zhu et al., "Temperature measurement of a horizontal cylinder in natural convection using a lateral shearing interferometer with a large shear amount," *Opt. Eng.* **54**(3), 034109 (2015).
17. M. M. Hossain and C. Shakher, "Temperature measurement in laminar free convective flow using digital holography," *Appl. Opt.* **48**(10), 1869–1877 (2009).
18. A. Ahadi, A. Khoshnevis, and M. Z. Saghir, "Windowed Fourier transform as an essential digital interferometry tool to study coupled heat and mass transfer," *Opt. Laser Technol.* **57**, 304–317 (2014).

19. Q. Wang et al., "Visual and quantitative measurement of the temperature distribution of heat conduction process in glass based on digital holographic interferometry," *J. Appl. Phys.* **111**(9), 093111 (2012).
20. A. Ahadi and M. Z. Saghir, "Determination of the glass wall effect in optical measurement of temperature in liquid using Mach–Zehnder interferometer," *Appl. Opt.* **54**(13), D74–D81 (2015).
21. B. Manukhin et al., "Optical diagnostics of the process of free liquid convection," *Opt. Spectrosc.* **119**(3), 392–397 (2015).
22. B. Skarman, K. Wozniak, and J. Becker, "Digital in-line holography for the analysis of bénard-convection," *Flow Meas. Instrum.* **10**(2), 91–97 (1999).
23. O. Dupont, J.-L. Dewandel, and J. C. Legros, "Use of electronic speckle pattern interferometry for temperature distribution measurements through liquids," *Opt. Lett.* **20**(17), 1824–1826 (1995).
24. Y. Zhang et al., "Real-time monitoring of the solution concentration variation during the crystallization process of protein-lysozyme by using digital holographic interferometry," *Opt. Express* **20**, 18415–18421 (2012).
25. J. Zhao et al., "Dynamic measurement for the solution concentration variation using digital holographic interferometry and discussion for the measuring accuracy," *Proc. SPIE* **8769**, 87690D (2013).
26. M. Takeda, H. Ina, and S. Kobayashi, "Fourier-transform method of fringe-pattern analysis for computer-based topography and interferometry," *J. Opt. Soc. Am.* **72**(1), 156–160 (1982).
27. G. Pedrini, H. J. Tiziani, and Y. Zou, "Digital double pulse-TV-holography," *Opt. Laser Eng.* **26**, 199–219 (1997).
28. G. Pedrini, S. Schedin, and H. J. Tiziani, "Lensless digital-holographic interferometry for the measurement of large objects," *Opt. Commun.* **171**, 29–36 (1999).
29. I. Thormählen, J. Straub, and U. Grigull, "Refractive index of water and its dependence on wavelength, temperature, and density," *J. Phys. Chem. Ref.* **14**, 933–945 (1985).
30. M. Abell and J. Braselton, *Introductory Differential Equations*, Elsevier Science, Amsterdam, Netherlands (2014).

Carlos Guerrero-Mendez received his MSc degree in engineering sciences from the Universidad Autónoma de Zacatecas (UAZ), México, in 2013. He is currently pursuing his PhD in engineering sciences at the UAZ. His research interests include holography techniques and phase retrieval methods.

Tonatiuh Saucedo Anaya graduated from the Centro de Investigaciones en Óptica A.C. (CIO) of México in 2006. His doctoral thesis was titled "Holografía Digital Pulsada con Endoscopio Rígido Para el Estudio de Deformaciones en Áreas de Difícil Acceso." Currently, he is a professor-researcher at the UAZ. His interests include digital holographic interferometry.

M. Araiza-Esquivel received her PhD in applied physics from Universidad Autónoma de San Luis Potosí (UASLP) in 2002. Currently, she is a professor-researcher at the UAZ. Her current research interests include digital holography.

Raúl E. Balderas-Navarro received his PhD in applied physics from the UASLP in 1998. Currently, he is a professor-researcher at the Instituto de Investigación en Comunicación Óptica at UASLP. His current research interests include optical processes in semiconductors.

Said Aranda-Espinoza studied his PhD at the Max Planck Institute of Colloids and Interfaces (MPICI). Currently, he is a professor-researcher at the Instituto de Física at UASLP. His current research interests include deformations of membranes.

Alfonso López-Martínez received his PhD from the UAZ. His doctoral thesis was titled "Diseño y análisis de un controlador vía modo deslizantes de alto orden aplicado a un sistema de potencia SMIB-SVC."

Carlos Olvera-Olvera recived his PhD from the Universidad Autónoma de Querétaro (UAQ). Currently, he is a professor-researcher at the UAZ. His current research interests include remote sensing and control systems.